

Closure of the Proterozoic Mozambique Ocean was instigated by a late Tonian plate reorganization event

Alan S. Collins^{1*}, Morgan L. Blades¹, Andrew S. Merdith², John D. Foden¹

¹*Tectonics and Earth Systems (TES), Department of Earth Sciences, The University of Adelaide, Adelaide, SA 5005, Australia.*

²*UnivLyon, Université Lyon 1, Ens de Lyon, CNRS, UMR 5276 LGL-TPE, F-69622, Villeurbanne, France*

**corresponding author*

alan.collins@adelaide.edu.au, Twitter @geoAlanC

morgan.blades@adelaide.edu.au,

andrew.merdith@univ-lyon1.fr

john.foden@adelaide.edu.au

This is a pre-print of a manuscript accepted for publication in *Communications Earth & Environment*

<https://www.nature.com/commsenv/>

Closure of the Proterozoic Mozambique Ocean was instigated by a late Tonian plate reorganization event

Alan S. Collins^{1*}, Morgan L. Blades¹, Andrew S. Merdith², John D. Foden¹

¹*Tectonics and Earth Systems (TES), Department of Earth Sciences, The University of Adelaide, Adelaide, SA 5005, Australia.*

²*UnivLyon, Université Lyon 1, Ens de Lyon, CNRS, UMR 5276 LGL-TPE, F-69622, Villeurbanne, France*

*corresponding author

alan.collins@adelaide.edu.au,

morgan.blades@adelaide.edu.au,

andrew.merdith@univ-lyon1.fr

john.foden@adelaide.edu.au

ABSTRACT

Plate reorganization events involve fundamental changes in lithospheric plate-motions and can influence the lithosphere-mantle system as well as both ocean and atmospheric circulation through bathymetric and topographic changes. Here, we compile published data to interpret the geological record of the Neoproterozoic Arabian-Nubian Shield and integrate this with a full-plate tectonic reconstruction. Our model reveals a plate reorganization event in the late Tonian period about 720 million years ago that changed plate-movement directions in the Mozambique Ocean. After the reorganization, Neoproterozoic India moved towards both the African cratons and Australia-Mawson and instigated the future amalgamation of central Gondwana about 200 million years later. This plate kinematic change is coeval with the break-up of the core of Rodinia between Australia-Mawson and Laurentia and Kalahari and Congo. We suggest the plate reorganization event caused the long-term shift of continents to the southern hemisphere and created a pan-northern hemisphere ocean in the Ediacaran.

INTRODUCTION

Plate tectonics is characterized by periods of gradual, broadly continuous, plate movement that are punctuated by relatively short times of plate reorganization^{1,2}. These are due to the consumption of an oceanic plate, the collision of two continents, the cessation of subduction,

34 or the break-up of a (super)continent^{3,4}. These events disturb the plate kinematic *status quo*
35 and force adjustments over the planet surface that affect ocean and atmospheric circulation
36 and have been linked to perturbations in the carbon cycle⁵, amongst other things. Identifying
37 and understanding plate reorganization events in deep time is only possible with full-plate
38 topological reconstructions. These are well developed for the Mesozoic and younger⁶, but
39 have only recently been proposed for the Palaeozoic^{7,8} and now Neoproterozoic eras^{9,10}.
40 These allow regional plate-tectonic induced phenomena to be understood in a global context.
41 Here we present an updated GPlates (www.gplates.org) model that uses recently published
42 geological data from the terranes of the Arabian Nubian Shield (ANS). By adding in
43 geological data from relic volcanic arcs into these full-plate topological reconstructions of the
44 ancient earth, we provide a new interpretation of the oceanic plate kinematic and dynamic
45 evolution of the Neoproterozoic Mozambique Ocean. This led to the southward journey of
46 Neoproterozoic India to collide against African Gondwana and the Australia-Mawson
47 continent¹¹ to form the kernel of Gondwana. This plate reorganization is coeval with the
48 opening of the Pacific Basin^{12,13} and directly precedes the cataclysmic climatic perturbations
49 of the Cryogenian.

50

51 **BACKGROUND**

52 Plate tectonics has been causally linked to the Cryogenian climate instability¹⁴⁻¹⁶, to the
53 coeval Neoproterozoic Oxygenation Event^{17,18}, to the biosphere tumult that included the
54 ecological takeover of eukaryote cells^{19,20} and, ultimately, to the evolution of metazoans^{21,22}.
55 The veracity of these hypotheses requires knowledge of the plate tectonic configuration and
56 kinematics through the Neoproterozoic, which is missing, as most attempted reconstructions
57 are ‘continental-drift’ models with no full-plate circuit attempted^{11,23}. A first attempt at a
58 full-plate topological model for 1000–520 Ma was recently published⁹. However, this model
59 focused predominantly on cratonic crust that had available palaeomagnetic data, and
60 consequently simplified many complex areas around Neoproterozoic active margins. Mallard
61 et al.²⁴ demonstrated that active margins control plate size and number, therefore also control
62 many of the parameters needed to understand the role of plate tectonics on broader earth
63 systems. The ANS was an active margin and one of these areas simplified in Merdith et al.⁹,
64 yet, it is one of the most critical for Neoproterozoic plate reconstructions as it is one of the
65 most extensive areas of new Neoproterozoic crust on the planet²⁵ (Fig. 1) and preserves
66 evidence of subduction from pre-1 Ga until the Ediacaran²⁶.

67

68 The end of the Proterozoic eon is marked by some of the most dramatic events in Earth's
69 history, with this period of time being characterised by extensive changes in seawater
70 chemistry demonstrated through the strontium, sulfur and carbon isotope records, large
71 climatic extremes, and preservation of the Ediacaran faunal assemblage and the explosion of
72 Cambrian fauna ²⁷. These global variations are concurrent with the amalgamation of
73 Gondwana, and the closure of the Mozambique Ocean; representing one of the major and
74 final Gondwana forming collisional zones ²⁸. As no in-situ oceanic crust exists before ca. 200
75 Ma, the remnants of this major ocean gateway are only preserved in relic arc-arc, arc-
76 continent and continent-continent collisional zones, within the East African Orogen (EAO).
77 The EAO is one of the largest orogens of the last billion years, which, in a reconstructed
78 Gondwana, extends from Turkey and the Levant, in the north to Mozambique, Madagascar,
79 Sri Lanka and East Antarctica in the south ²⁹. Along strike, the orogen is divided into two.
80 The Mozambique Belt lies in the south and is a tract of largely older continental crust,
81 extensively deformed and metamorphosed in the Neoproterozoic/Cambrian ³⁰. The ANS
82 makes up the north of the orogen ²⁶. The ANS, and adjacent Gondwanan rocks in North
83 Africa and from east Arabia to NW India preserve the evidence we use to reconstruct the
84 plate tectonic circuit as Neoproterozoic India converged and finally collided with the African
85 parts of Gondwana ²⁶.

86

87 **RESULTS AND DISCUSSION**

88

89 **MODEL CONSTRAINTS**

90 In this paper, we use previously published geological data to constrain our full-plate
91 topological model for the evolution and closure of the Mozambique Ocean and the
92 amalgamation of central Gondwana. The full-plate model is based on geological and
93 paleomagnetic data and is part of the first published self-consistent model of global plate
94 tectonics over the last billion years ¹⁰. We emphasize that this is a model, and although we
95 argue that it is best represents the geological and paleomagnetic data available in 2021, it is
96 not a unique solution and is subject to improvement with more data and better interpretations.
97 The model, however, does present interesting implications for the progression of plate
98 tectonics over this time, the distribution of plates, of continents and oceans and leads to
99 hypotheses for plate-tectonic influence of earth-surface systems that we begin to explore in
100 this paper.

101 The ANS is laced with suture zones that represent collisions between different terranes as
102 subduction zones consumed the intervening oceanic crust (Fig. 1). A dramatic feature of the
103 region is that pre-715 Ma sutures are aligned approximately ninety degrees from post-715 Ma
104 sutures^{26,31}. This observation reflects a major change in plate convergence direction and we
105 use this as the start of a higher-order reconstruction of this region in a full-plate context.

106 **The Mozambique Ocean, Azania and Afif-Abas**

107 The Mozambique Ocean closed as Neoproterozoic India converged on the African parts of
108 Gondwana (Kalahari, Congo, Sahara) to form central Gondwana²⁹. The East African Orogen
109 resulted from the collision between these major continents and amalgams of smaller terranes,
110 during the Neoproterozoic to early Cambrian. Sandwiched within the EAO lies a broad band
111 of Archean to Paleoproterozoic crust that was identified by Collins and Windley³² as a
112 microcontinent (subsequently named 'Azania'), whose remains are found in southern India,
113 central Madagascar, Somalia, eastern Ethiopia and Arabia (Fig. 1). In Yemen, the Al-Mafid
114 Terrane is correlated with Azania³² and this is separated from a second pre-Neoproterozoic
115 terrane called the Abas Terrane by a Neoproterozoic arc terrane (the Al Bayda terrane).
116 Because of this, Collins and Windley³² suggested that a second microcontinent existed that
117 they called Afif-Abas due to the continuation of the Abas terrane into Saudi Arabia as the
118 Afif Terrane.

119

120 Azania, and Afif-Abas, are interpreted to have collided with the eastern margins of the Congo
121 craton and Saharan Metacraton by approximately 630 Ma to form the East African Orogeny
122 *sensu stricto*. A younger orogeny (ca. 570–520 Ma), was interpreted to represent the final
123 collision between India and the amalgamated Africa/Arabia and called the Malagasy orogeny
124¹¹.

125

126 **The Eastern Margin of the EAO (NW India to Oman)**

127 The easternmost margin of the northern East African Orogen is the boundary between the
128 Mesoproterozoic terranes of India and the Stenian–Tonian crust that extends west from the
129 Delhi-Aravalli Orogen. This has been interpreted to be the eastern margin of the northern
130 East African Orogen. During the Stenian and Tonian, progressive arc accretion of volcanic
131 arc rocks onto the NW margin of Neoproterozoic India occurred; extending into the basement
132 rocks of Pakistan and the inliers of Oman^{33,34}. This was later covered by an extensive
133 Cryogenian-Ediacaran passive margin succession, with comparable sequences continuing
134 into the Cambrian³⁵.

135

136 **The Arabian Nubian Shield**

137 The ANS is dominated by low grade volcano-sedimentary sequences and associated plutonic
138 and ophiolitic remnants. The tectonic history of the ANS is complicated and preserves a
139 complex mix of terranes, accreted arcs that record subduction polarity reversals that are
140 reviewed and summarised in a number of papers^{26,31}. There are no reliable paleomagnetic
141 data available to constrain these blocks, so we have constrained their positions by their
142 relation to each other and through plate kinematic constraints.

143

144 The oldest terrane in the ANS is the late Mesoproterozoic Sa'al Metamorphic complex (1.03–
145 1.02 Ga) in Sinai, marking the initiation of magmatism in the northern-most ANS^{36,37} (Fig.
146 1). The location of this Stenian terrane in the reconstruction is uncertain, but coeval
147 subduction-magmatism occurred within the Saharan Metacraton (see below).

148

149 The Tonian to Cryogenian history of the ANS is marked by formation of oceanic volcanic
150 arcs and continental volcanic arcs built on Azanian (or Afif-Abas) crust that amalgamated to
151 form a larger intra-Mozambique ocean terrane separate from both Neoproterozoic India and
152 African Gondwanan continents. A number of terranes in the ANS are correlated as
153 equivalents, separated by the opening of the Red Sea, from south to north, these are the Asir
154 and Tokar/Barka terranes, the Haya and Jiddah terranes, the Hijaz and Gabgaba/Gebeit
155 terranes, and the Eastern Desert and Midyan terranes²⁶. It is unclear whether the combined
156 Asir-Tokar/Barka terrane and Haya-Jiddah terranes were ever on separate plates as, in Saudi
157 Arabia, no clear suture is seen between them. In SE Sudan and Eritrea, the Barka suture does
158 appear as the site of ocean closure, so these may form a complex middle Tonian amalgam.

159

160 The older, Tonian to earliest Cryogenian, amalgamation history of the ANS is marked by
161 approximately ENE-WSW oriented sutures (present orientation) between juvenile
162 Neoproterozoic ocean-arc terranes. The oldest of these sutures is between the Jiddah-Haya
163 and Gabgaba/Gebeit-Hijaz terranes (the Bi'r Umq–Nakasib suture), which is dated at ca.
164 780–750 Ma²⁶. This suture created the kernel of a late Tonian microcontinent. The Midyan-
165 Eastern Desert collided with this kernel ca. 715 Ma along the Yanbu-Sol Hamed suture³¹.
166 Both of these sutures evolved from SE-dipping subduction zones³¹.

167

168 The older ENE-WSW sutures are bound by younger NNW-SSE Cryogenian to Ediacaran
169 sutures and terranes that represent a fundamental kinematic change in Mozambique Ocean
170 subduction. The oldest of these is the 680–640 Ma Nabitah suture, which forms the eastern
171 margin of the intra-Mozambique Ocean island-arc terrane microcontinent (discussed above),
172 against Tonian–Cryogenian continental arcs built on the Afif-Abas microcontinent. This now
173 enlarged Cryogenian Afif-Abas microcontinent collided with the active margin of the Sahara
174 Metacraton along the Sudanese Keraf Suture. This collision occurred in late Cryogenian to
175 early Ediacaran times (ca. 650–580 Ma)³⁸. Further to the east, in the most easterly exposed
176 terrane, the Saudi Ar Rayn Terrane, juvenile calc-alkaline magmatism stretches from ca. 690
177 Ma to 615 Ma³⁹. Turbiditic sediment deposition in the Ad Dawadimi basin that separates the
178 Ar Rayn Terrane from the Afif-Abas microcontinent continued until at least 620 Ma, but was
179 locally intruded by ca. 630 Ma adakitic magmas⁴⁰. This sequence was metamorphosed to
180 greenschist-facies grades at ca. 620 Ma⁴¹. Further east still, broad N–S magnetic highs,
181 beneath the Arabian Phanerozoic sedimentary sequence⁴², suggest younger arc terranes now
182 buried beneath the Rub al-Khali Basin. The transition to post-tectonic magmatism within the
183 eastern terranes of the ANS begins from 605 Ma³⁹ and pull-apart basins developed along the
184 large strike-slip faults that cut the region⁴³. Post-tectonic magmatism begins in western
185 Ethiopia at ca. 572 Ma⁴⁴.

186

187 The final collision between Neoproterozoic India and the, by then amalgamated,
188 Azania/Congo Craton occurred at ca. 570–540 Ma, closing the final strand of the
189 Mozambique Ocean^{11,28}. This suture lies beneath the Phanerozoic cover between the exposed
190 Saudi and Yemen basement and Mirbat in SW Oman. It appears to be imaged by shear-wave
191 anisotropy variations seen directly west of Mirbat⁴⁵. In western Oman, latest Ediacaran–
192 Cambrian deformation is seen in the subsurface, its limit is known as the Western
193 Deformation Front and the deformation associated with this is known as the ‘Angudan event’.
194 The sub-Rub al-Khali suture has been traced south within reconstructed Gondwana to
195 Madagascar where it has been correlated with the Antsaba shear zone of NW Madagascar⁴⁶,
196 the Betsimisaraka suture³² and into the Palghat–Cauvery Suture of southern India⁴⁷. This
197 Palghat–Betsimisaraka–Antsaba–Western Deformation Front suture represents the final
198 suture of the Mozambique Ocean^{9,11}.

199

200 **The Western Margin of the EAO (the eastern Saharan Metacraton)**

201 The Saharan Metacraton is still very poorly known, but extensive late Mesoproterozoic
202 subduction-related magmatism is found in Chad and west and north Sudan ⁴⁸. To the west of
203 this, in eastern Sudan and western Ethiopia magmatism associated with early Neoproterozoic
204 subduction characterizes terranes that are thought to have formed over westward dipping
205 subduction zones ^{44,49}. This longevity of subduction, which also includes that seen in the
206 Sinai ^{36,37}, demonstrates that the EAO extends back into the Stenian, or even earlier, when
207 terrane accretion and subduction-zone magmatism initiated against the Paleoproterozoic
208 kernel of the ‘metacraton’. The NE margin of the Congo Craton, in Uganda, preserves
209 orogenesis that begins with Tonian subduction-zone magmatism in the Karamoja Belt that is
210 coeval with terranes in Sudan ⁵⁰.

211

212 **A LATE TONIAN PLATE RECONFIGURATION**

213

214 The model presented here (Fig. 2) is developed from the reconstruction of Merdith et al. ⁹.
215 Details of both geological and paleomagnetic data used to constrain cratonic configurations,
216 positions and motions are provided therein. Here, data and observations discussed above for
217 the terranes of northern Africa, Arabia and NW India have been integrated ¹⁰. These define a
218 marked change in Mozambique Ocean subduction kinematics at ca. 720 Ma, from a
219 predominately N–S to E–W striking subduction system (Fig. 2). The timing of these observed
220 changes are broadly coeval with the start of Neoproterozoic India’s southern progression
221 from polar regions to lower latitudes ^{29,51,52} and we suggest that they represent a plate
222 reorganization in this hemisphere. This kinematic shift is coeval with sedimentological and
223 kinematic estimates for the breakup of the core of Rodinia. The ancestral Pacific basin is
224 constrained to open before 725 Ma based on kinematic constraints ¹² and separation of the
225 Kalahari and Congo continents is also consistent with voluminous magmatism along the
226 southern Congo margin at ca. 750 Ma ⁵³. This late Tonian plate reorganization heralds the
227 start of a shift of continental crust away from the northern hemisphere into the southern
228 hemisphere (Figs. 2 and 3). This narrows, then eventually closes the equatorial Mozambique
229 Ocean. The model implies that most continental blocks were concentrated in the southern
230 hemisphere in the Late Neoproterozoic (Fig. 3). If this reflects the real distribution, then it
231 would have interesting consequences for ocean/atmosphere circulation. One possible effect
232 would be to compartmentalize ocean gyres in the southern hemisphere, while removing
233 obstacles for hemispherical circulation in the northern hemisphere (Fig. 2). This shift from bi-
234 hemisphere continent distribution towards a world with a pan-northern hemisphere ocean and

235 continents concentrated in the southern hemisphere coincides with end of whole-earth
236 glaciations that characterize the middle Neoproterozoic. In contrast to the Sturtian and
237 Marinoan whole-earth glaciations, Ediacaran glaciations, such as the Gaskiers glaciation,
238 appear more regional in scale ^{15,54}. Williams and Schmidt ⁵⁵ hypothesized that the mid-
239 Ediacaran Shuram/Wonoka negative carbon isotope anomaly represents an unprecedented
240 perturbation of the world ocean. We speculate that the plate tectonic driven bifurcation of the
241 planet into continent and ocean latitudinal hemispheres may be a major control on this
242 oceanic perturbation and climate switch—a consequence of the late Tonian plate
243 reorganization.

244

245 **ACKNOWLEDGMENTS**

246 ASC is supported by Australian Research Council grants FT120100340 and with MLB and
247 JDF are funded by LP160101353, with the support of the Northern Territory Geological
248 Survey, Origin Energy, Santos Ltd and Imperial Oil and Gas. ASM is supported by the Deep
249 Energy Community of the Deep Carbon Observatory. We thank Anthony Pivarunas and an
250 anonymous reviewer who improved the manuscript.

251

252 **METHODS**

253 This manuscript is based on a full-plate tectonic reconstruction of the last billion years that
254 has been developed on the open access software GPlates (www.gplates.org). All GPlates files
255 needed to reconstruct the model are available here—<https://zenodo.org/record/3647901>. The
256 methodology for constructing full-plate tectonic reconstructions are detailed in Merdith et al.
257 ¹⁰ and also in Domeier and Torsvik ⁵⁶. Computation of latitudinal surface area was done using
258 pyGplates (www.pygplates.org). To extract the latitudinal distribution of continent area, we
259 first created a global equal-area mesh. We then used a grid-intersection between the nodes of
260 the mesh and the polygons of the plate model that represent continental crust to estimate the
261 area of crust at each latitude. These were summed for each timestep to create an array from
262 1000–520 Ma of the latitudinal distribution of crust on the earth

263

264 **DATA AVAILABILITY**

265 Data derived from the full-plate reconstructions used here to evaluate the latitudinal
266 distribution of continental crust through time are publically available at

267 https://github.com/amer7632/Collins_2021_Geology_palaeolat

268

269 **CODE AVAILABILITY**

270 The code used to calculate and construct Figure 3 it is available here:

271 https://github.com/amer7632/Collins_2021_Geology_palaeolat

272

273 **REFERENCES**

274

- 275 1 Gordon, R. G. & Jurdy, D. M. Cenozoic Global Plate Motions. *J Geophys Res-Solid*
276 **91**, 2389-2406, doi:DOI 10.1029/JB091iB12p12389 (1986).
- 277 2 Muller, R. D. *et al.* Ocean Basin Evolution and Global-Scale Plate Reorganization
278 Events Since Pangea Breakup. *Annual Review of Earth and Planetary Sciences* **44**,
279 107-138, doi:10.1146/annurev-earth-060115-012211 (2016).
- 280 3 Austermann, J. *et al.* Quantifying the forces needed for the rapid change of Pacific
281 plate motion at 6 Ma. *Earth and Planetary Science Letters* **307**, 289-297,
282 doi:10.1016/j.epsl.2011.04.043 (2011).
- 283 4 Whittaker, J. M. *et al.* Major Australian-Antarctic plate reorganization at Hawaiian-
284 Emperor bend time. *Science* **318**, 83-86, doi:10.1126/science.1143769 (2007).
- 285 5 Louis-Schmid, B. *et al.* Detailed record of the mid-Oxfordian (Late Jurassic) positive
286 carbon-isotope excursion in two hemipelagic sections (France and Switzerland): A
287 plate tectonic trigger? *Palaeogeography Palaeoclimatology Palaeoecology* **248**, 459-
288 472, doi:10.1016/j.palaeo.2007.01.001 (2007).
- 289 6 Muller, R. D. *et al.* A Global Plate Model Including Lithospheric Deformation Along
290 Major Rifts and Orogens Since the Triassic. *Tectonics* **38**, 1884-1907,
291 doi:10.1029/2018tc005462 (2019).
- 292 7 Domeier, M. A plate tectonic scenario for the Iapetus and Rheic oceans. *Gondwana*
293 *Research* **36**, 275-295, doi:10.1016/j.gr.2015.08.003 (2016).
- 294 8 Domeier, M. & Torsvik, T. H. Plate tectonics in the late Paleozoic. *Geoscience*
295 *Frontiers* **5**, 303-350, doi:10.1016/j.gsf.2014.01.002 (2014).
- 296 9 Merdith, A. S. *et al.* A full-plate global reconstruction of the Neoproterozoic.
297 *Gondwana Research* **50**, 84-134, doi:10.1016/j.gr.2017.04.001 (2017).
- 298 10 Merdith, A. S. *et al.* Extending full-plate tectonic models into deep time: Linking the
299 Neoproterozoic and the Phanerozoic. *Earth-Science Reviews* **214**, 103477,
300 doi:https://doi.org/10.1016/j.earscirev.2020.103477 (2021).
- 301 11 Collins, A. & Pisarevsky, S. Amalgamating eastern Gondwana: The evolution of the
302 Circum-Indian Orogens. *Earth-Science Reviews* **71**, 229-270,
303 doi:10.1016/j.earscirev.2005.02.004 (2005).
- 304 12 Merdith, A. S., Williams, S. E., Muller, R. D. & Collins, A. S. Kinematic constraints
305 on the Rodinia to Gondwana transition. *Precambrian Research* **299**, 132-150,
306 doi:10.1016/j.precamres.2017.07.013 (2017).
- 307 13 Lloyd, J. C. *et al.* Neoproterozoic geochronology and provenance of the Adelaide
308 Superbasin. *Precambrian Research* **350**, 105849,
309 doi:10.1016/j.precamres.2020.105849 (2020).
- 310 14 Gernon, T. M., Hincks, T. K., Tyrrell, T., Rohling, E. J. & Palmer, M. R. Snowball
311 Earth ocean chemistry driven by extensive ridge volcanism during Rodinia breakup.
312 *Nature Geoscience* **9**, 242-U283, doi:10.1038/Ngeo2632 (2016).
- 313 15 Hoffman, P. F. *et al.* Snowball Earth climate dynamics and Cryogenian geology-
314 geobiology. *Sci Adv* **3**, e1600983, doi:10.1126/sciadv.1600983 (2017).

- 315 16 Sobolev, S. V. & Brown, M. Surface erosion events controlled the evolution of plate
316 tectonics on Earth. *Nature* **570**, 52+, doi:10.1038/s41586-019-1258-4 (2019).
- 317 17 Li, C., Cheng, M., Zhu, M. & Lyons, T. W. Heterogeneous and dynamic marine shelf
318 oxygenation and coupled early animal evolution. *Emerging Topics in Life Sciences* **2**,
319 279–288, doi:https://doi.org/10.1042/ETLS20170157 (2018).
- 320 18 Williams, J. J., Mills, B. J. W. & Lenton, T. M. A tectonically driven Ediacaran
321 oxygenation event. *Nat Commun* **10**, 2690, doi:10.1038/s41467-019-10286-x (2019).
- 322 19 Lenton, T. M., Boyle, R. A., Poulton, S. W., Shields-Zhou, G. A. & Butterfield, N. J.
323 Co-evolution of eukaryotes and ocean oxygenation in the Neoproterozoic era. *Nature*
324 *Geoscience* **7**, 257-265, doi:10.1038/ngeo2108 (2014).
- 325 20 Brocks, J. J. *et al.* The rise of algae in Cryogenian oceans and the emergence of
326 animals. *Nature* **548**, 578+, doi:10.1038/nature23457 (2017).
- 327 21 Sahoo, S. K. *et al.* Ocean oxygenation in the wake of the Marinoan glaciation. *Nature*
328 **489**, 546-549, doi:10.1038/nature11445 (2012).
- 329 22 McKenzie, N. R., Hughes, N. C., Gill, B. C. & Myrow, P. M. Plate tectonic influences
330 on Neoproterozoic-early Paleozoic climate and animal evolution. *Geology* **42**, 127-
331 130, doi:10.1130/G34962.1 (2014).
- 332 23 Li, Z. X. *et al.* Assembly, configuration, and break-up history of Rodinia: A synthesis.
333 *Precambrian Research* **160**, 179-210, doi:10.1016/j.precamres.2007.04.021 (2008).
- 334 24 Mallard, C., Coltice, N., Seton, M., Muller, R. D. & Tackley, P. J. Subduction
335 controls the distribution and fragmentation of Earth's tectonic plates. *Nature* **535**, 140-
336 +, doi:10.1038/nature17992 (2016).
- 337 25 Stern, R. A. Crustal evolution in the East African Orogen: a neodymium isotopic
338 perspective. *Journal Of African Earth Sciences* **34**, 109-117 (2002).
- 339 26 Johnson, P. R. *et al.* Late Cryogenian-Ediacaran history of the Arabian-Nubian
340 Shield: A review of depositional, plutonic, structural, and tectonic events in the
341 closing stages of the northern East African Orogen. *Journal of African Earth Sciences*
342 **61**, 167-232, doi:10.1016/j.jafrearsci.2011.07.003 (2011).
- 343 27 Halverson, G. P., Hurtgen, M., Porter, S. M. & Collins, A. S. in *Events at the*
344 *Precambrian-Cambrian boundary: a focus on southwestern Gondwana* (eds C.
345 Gaucher, A. Sial, G.P Halverson, & H. Frimmel) (Elsevier, Developments in
346 Precambrian Geology, 2010).
- 347 28 Schmitt, R. d. S., Fragoso, R. d. A. & Collins, A. S. in *Geology of Southwest*
348 *Gondwana* (eds Siegfried Siegesmund, Miguel A. S. Basei, Pedro Oyhantçabal, &
349 Sebastian Oriolo) 411-432 (Springer International Publishing, 2018).
- 350 29 Meert, J. G. A synopsis of events related to the assembly of eastern Gondwana.
351 *Tectonophysics* **362**, 1-40 (2003).
- 352 30 Fritz, H. *et al.* Orogen styles in the East Africa Orogens: A review of the
353 Neoproterozoic to Cambrian Tectonic Evolution. *Journal of African Earth Sciences*
354 **86**, 65-106 (2013).
- 355 31 Robinson, F. A., Foden, J. D. & Collins, A. S. Geochemical and isotopic constraints
356 on island arc, synorogenic, post-orogenic and anorogenic granitoids in the Arabian
357 Shield, Saudi Arabia. *Lithos* **220**, 97-115, doi:10.1016/j.lithos.2015.01.021 (2015).
- 358 32 Collins, A. & Windley, B. The tectonic evolution of central and northern Madagascar
359 and its place in the final assembly of Gondwana. *Journal of Geology* **110**, 325-339,
360 doi:10.1086/339535 (2002).
- 361 33 Alessio, B. L. *et al.* Origin and tectonic evolution of the NE basement of Oman: a
362 window into the Neoproterozoic accretionary growth of India? *Geological Magazine*
363 **155**, 1150-1174, doi:10.1017/S0016756817000061 (2018).

- 364 34 Blades, M. L. *et al.* Unravelling the Neoproterozoic accretionary history of Oman,
365 using an array of isotopic systems in zircon. *Journal of the Geological Society*,
366 jgs2018-2125, doi:10.1144/jgs2018-125 (2019).
- 367 35 Cozzi, A., Rea, G. & Craig, J. From global geology to hydrocarbon exploration:
368 Ediacaran-Early Cambrian petroleum plays of India, Pakistan and Oman. *Geological*
369 *Society, London, Special Publications* **366**, 131-162, doi:10.1144/sp366.14 (2012).
- 370 36 Be'eri-Shlevin, Y., Eyal, M., Eyal, Y., Whitehouse, M. J. & Litvinovsky, B. The Sa'al
371 volcano-sedimentary complex (Sinai, Egypt): A latest Mesoproterozoic volcanic arc
372 in the northern Arabian Nubian Shield. *Geology* **40**, 403-406, doi:10.1130/G32788.1
373 (2012).
- 374 37 Eyal, M., Be'eri-Shlevin, Y., Eyal, Y., Whitehouse, M. J. & Litvinovsky, B. Three
375 successive Proterozoic island arcs in the Northern Arabian-Nubian Shield: Evidence
376 from SIMS U-Pb dating of zircon. *Gondwana Research* **25**, 338-357,
377 doi:10.1016/j.gr.2013.03.016 (2014).
- 378 38 Abdelsalam, M. G. *et al.* The Neoproterozoic Keraf Suture in NE Sudan: sinistral
379 transpression along the eastern margin of West Gondwana. *Journal of Geology* **106**,
380 133-147 (1998).
- 381 39 Doebrich, J. L. *et al.* Geology and metalogeny of the Ar Rayn terrane, eastern Arabian
382 shield: Evolution of a Neoproterozoic continental-margin arc during assembly of
383 Gondwana within the East African orogen. *Precambrian Research* **158**, 17-50 (2007).
- 384 40 Cox, G. M., Foden, J. & Collins, A. S. Late Neoproterozoic adakitic magmatism of
385 the eastern Arabian Nubian Shield. *Geoscience Frontiers* **10**, 1981-1992,
386 doi:10.1016/j.gsf.2017.12.006 (2019).
- 387 41 Cox, G. M. *et al.* Ediacaran terrane accretion within the Arabian-Nubian Shield.
388 *Gondwana Research* **21**, 341-352, doi:10.1016/j.gr.2011.02.011 (2012).
- 389 42 Johnson, P. R. & Stewart, I. C. F. Magnetically inferred basement structure in central
390 Saudi Arabia. *Tectonophysics* **245**, 37-52 (1995).
- 391 43 Nettle, D. *et al.* A middle-late Ediacaran volcano-sedimentary record from the eastern
392 Arabian-Nubian shield. *Terra Nova* **26**, 120-129, doi:10.1111/ter.12077 (2014).
- 393 44 Blades, M. L. *et al.* Age and hafnium isotopic evolution of the Didesa and Kemashi
394 Domains, western Ethiopia. *Precambrian Research* **270**, 267-284,
395 doi:10.1016/j.precamres.2015.09.018 (2015).
- 396 45 Al-Lazki, A. *et al.* Upper mantle anisotropy of southeast Arabia passive margin [Gulf
397 of Aden northern conjugate margin], Oman. *Arab J Geosci* **5**, 925-934,
398 doi:10.1007/s12517-011-0477-2 (2012).
- 399 46 Armistead, S. E. *et al.* Evolving Marginal Terranes During Neoproterozoic
400 Supercontinent Reorganization: Constraints From the Bemarivo Domain in Northern
401 Madagascar. *Tectonics* **38**, 2019-2035, doi:10.1029/2018tc005384 (2019).
- 402 47 Collins, A. S. *et al.* Passage through India: the Mozambique Ocean suture, high-
403 pressure granulites and the Palghat-Cauvery shear zone system. *Terra Nova* **19**, 141-
404 147, doi:10.1111/j.1365-3121.2007.00729.x (2007).
- 405 48 de Wit, M. J. & Linol, B. in *Geology and Resource Potential of the Congo Basin*
406 (eds Maarten J. de Wit, François Guillocheau, & Michiel C. J. de Wit) 19-37
407 (Springer Berlin Heidelberg, 2015).
- 408 49 Blades, M. L., Foden, J., Collins, A. S., Alemu, T. & Woldetinsae, G. The origin of
409 the ultramafic rocks of the Tulu Dimtu Belt, western Ethiopia - do they represent
410 remnants of the Mozambique Ocean? *Geological Magazine* **156**, 62-82,
411 doi:10.1017/S0016756817000802 (2019).

- 412 50 Westerhof, A. B. P. *et al.* Geology and Geodynamic Development of Uganda with
 413 Explanation of the 1:1,000,000 Scale Geological Map. 387 (Geological Survey of
 414 Finland, 2014).
- 415 51 Meert, J. G. *et al.* Precambrian crustal evolution of Peninsular India: A 3.0 billion
 416 year odyssey. *Journal of Asian Earth Sciences* **39**, 483-515, doi:DOI
 417 10.1016/j.jseaes.2010.04.026 (2010).
- 418 52 Powell, C. M. & Pisarevsky, S. A. Late Neoproterozoic assembly of East Gondwana.
 419 *Geology* **30**, 3-6 (2002).
- 420 53 Hoffman, P. F., Hawkins, D. P., Isachsen, C. E. & Bowring, S. A. Precise U-Pb zircon
 421 ages for early Damaran magmatism in the Summas Mountains and Welwitschia Inlier,
 422 northern Damara belt, Namibia. *Communications of the Geological Survey of*
 423 *Namibia* **11**, 47–52 (1996).
- 424 54 Pu, J. P. *et al.* Dodging snowballs: Geochronology of the Gaskiers glaciation and the
 425 first appearance of the Ediacaran biota. *Geology* **44**, 955-958, doi:10.1130/g38284.1
 426 (2016).
- 427 55 Williams, G. E. & Schmidt, P. W. Shuram-Wonoka carbon isotope excursion:
 428 Ediacaran revolution in the world ocean's meridional overturning circulation.
 429 *Geoscience Frontiers* **9**, 391-402, doi:10.1016/j.gsf.2017.11.006 (2018).
- 430 56 Domeier, M. & Torsvik, T. H. Full-plate modelling in pre-Jurassic time. *Geological*
 431 *Magazine* **156**, 261-280, doi:10.1017/S0016756817001005 (2019).
- 432 57 Cox, G. M. *et al.* South Australian U-Pb zircon (CA-ID-TIMS) age supports globally
 433 synchronous Sturtian deglaciation. *Precambrian Research* **315**, 257-263,
 434 doi:10.1016/j.precamres.2018.07.007 (2018).
- 435 57 Macdonald, F. A. *et al.* Calibrating the Cryogenian. *Science* **327**, 1241-1243,
 436 doi:10.1126/science.1183325 (2010).

437

438 **FIGURE CAPTIONS**

439

440 **Figure 1:** Map of present northern Indian Ocean region.

441 **Legend:** Showing the distribution of juvenile Stenian–Ediacaran crust, pre-Stenian exposed
 442 crust, pre-Stenian exposed crust reworked thermally and structurally during the
 443 Neoproterozoic, and Proterozoic sedimentary basins in NE Africa, Arabia and the Indian
 444 subcontinent. The late Tonian plate reconfiguration is represented by the notable change from
 445 pre-720 Ma, approximately NE-SW sutures to post-720 Ma, approximately NNW-SSE
 446 striking sutures. MB = Mozambique Belt, NED = Northern Eastern Desert, CED = Central
 447 Eastern Desert, SED = South Eastern Desert.

448

449 **Figure 2:** Global full-plate topological reconstructions.

450 **Legend:** a) 800 Ma, b) 750 Ma, c) 700 Ma, d) 600 Ma modified from Merdith *et al.* ^{9,10},
 451 focusing on detail within the ANS. A-A = Afif-Abas, Am = Amazonia, ANS = Arabian-
 452 Nubian Shield terrane, Az = Azania, Ba = Baltic, Bo = Borborema, Bu = Butana, C = Congo,
 453 Ca = Cathaysia, Ch = Chortis, DML = Dronning Maud Land, G = Greenland, H = Hoggar, I

454 = Neoproterozoic India, K = Kalahari, L = Laurentia, Ma = Mawson, NAC = North
455 Australian Craton, N-B = Nigeria-Benin, NC = North China, O = Oman, Pp = Paranapanema,
456 R = Rayner, RDLP = Rio de la Plata, S = Seychelles, SM = Sahara Metacraton, SF = Saõ
457 Francisco, SMC = Sa'al Metamorphic Complex, Sr = Sri Lanka, Si = Siberia, SAC = South
458 Australian/West Australian Craton, SES = South Ethiopian Shield, Ta = Tarim, WAC = West
459 African Craton, WES = West Ethiopian Shield, Yg = Yangtze. Colours refer to modern
460 continents that the terranes now make up: Red = Asia, Blue = Africa, Gold = South America,
461 Green = Europe, Yellow = North America, Purple = Australia, Teal = Antarctica, Lilac =
462 India, Madagascar and eastern Arabia. Blue dashed lines indicate schematic ocean currents.
463

464 **Figure 3:** Latitudinal distribution of continental crust with respect to time.

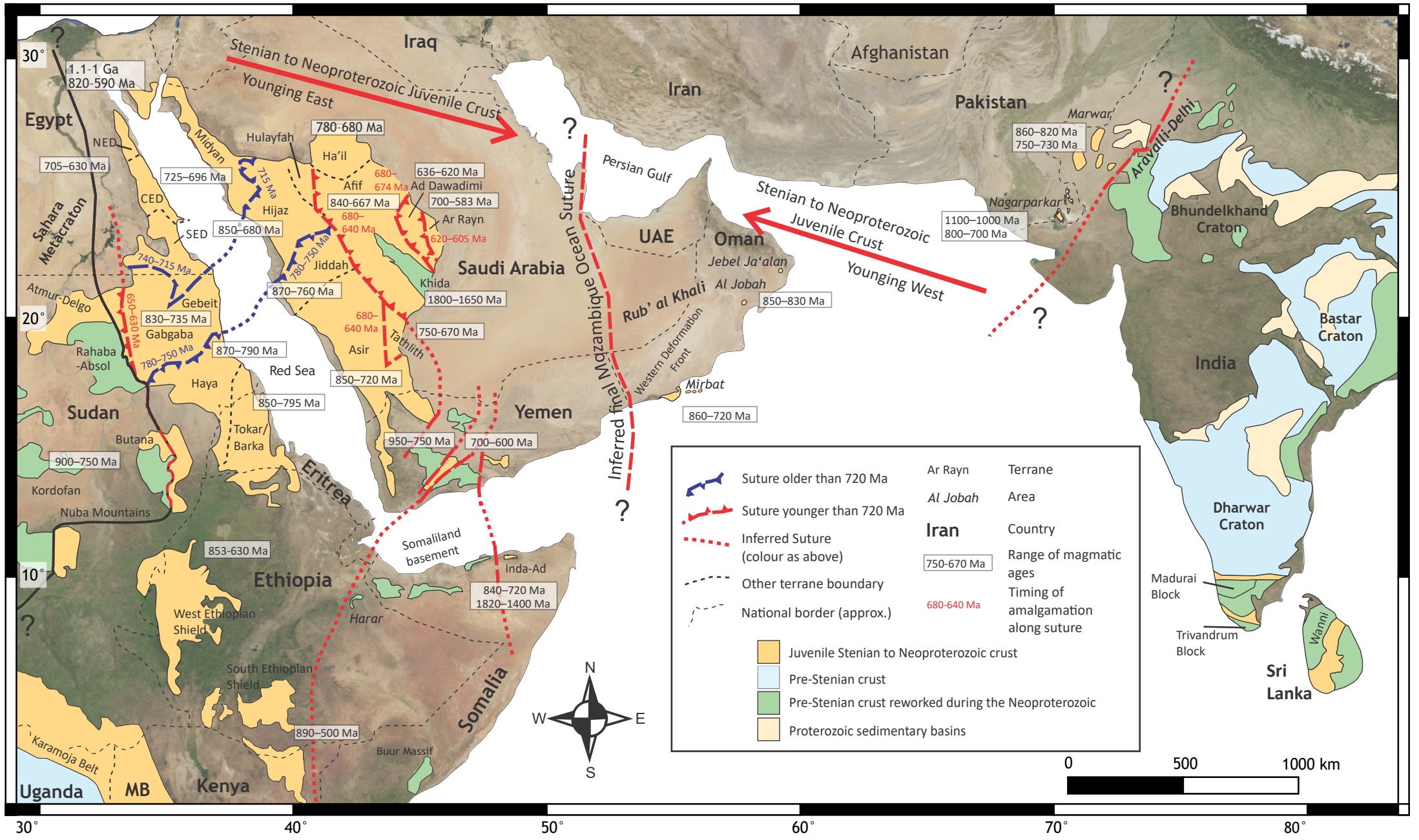
465 **Legend:** a) Percentage of continental crust in either hemisphere as a function of time. Sturtian
466 717–663 Ma, ^{57,58}, Marinoan 645–635 Ma, ¹⁵ and Gaskiers 579 Ma, ⁵⁴ glacial durations
467 indicated. b) Histograms of latitudinal distribution of continental area with respect to time
468 (Ma). Both as implied in Merdith et al. ¹⁰. If these models reflect reality, the late Tonian sees
469 the beginning of a long-term trend in continental crust moving to southern latitudes, first into
470 tropical regions through the Cryogenian, promoting a high albedo world. The Ediacaran sees
471 a shift to lower latitudes, which would suppress albedo. C = Cambrian.
472

473 AUTHOR CONTRIBUTIONS

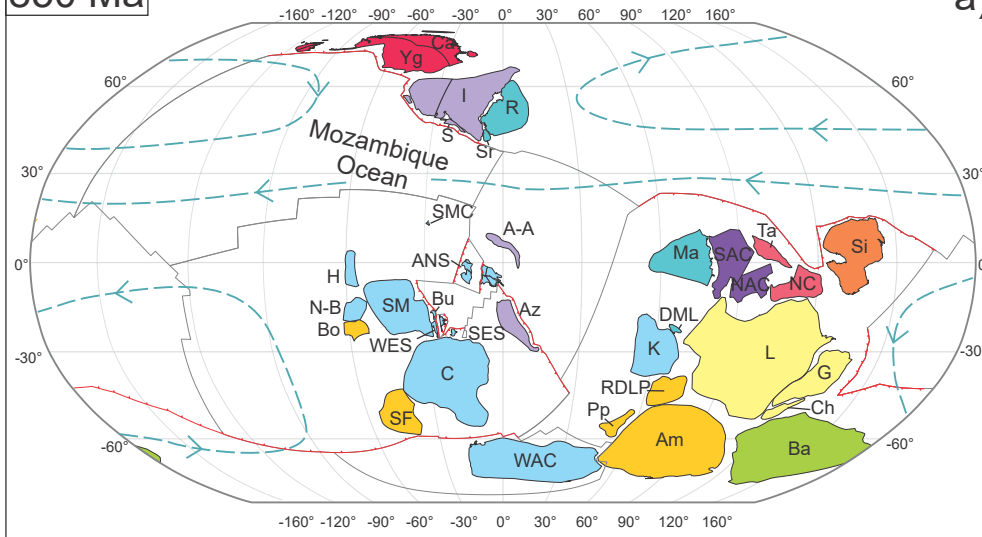
474
475 A.S.C., M.L.B. and J.D.F. conceived of and initiated the project. A.S.M. built the full-plate
476 reconstruction. A.S.C. and M.L.B. co-wrote the first draft of the paper. M.L.B. and A.S.M.
477 interpreted the data. All authors edited, revised and reviewed the manuscript.
478

479 COMPETETING INTERESTS

480
481 The authors declare no competing interests

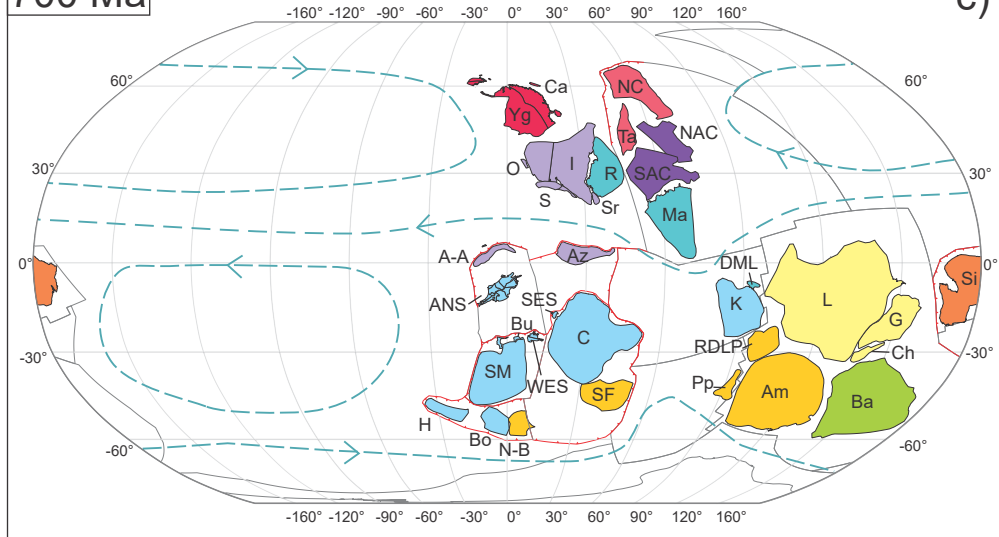


850 Ma



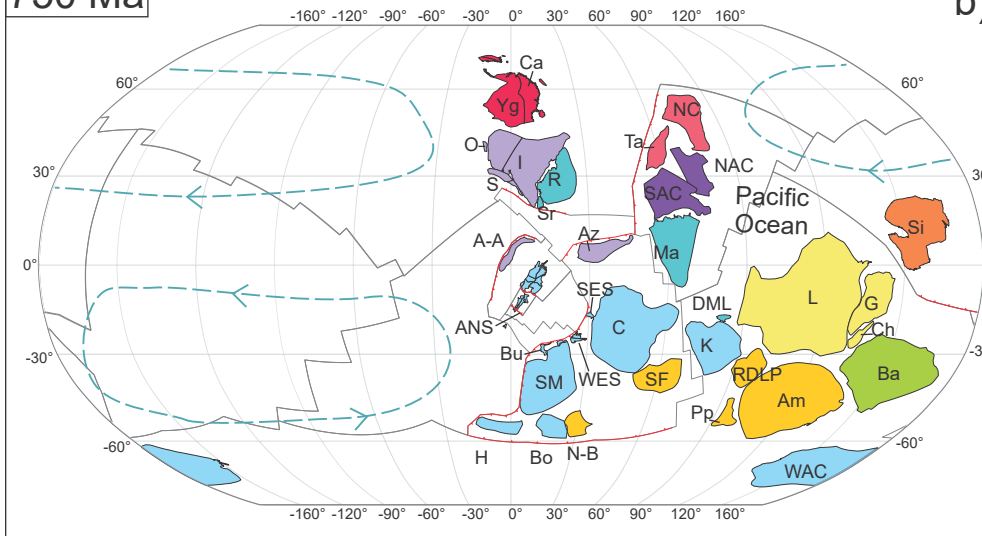
a)

700 Ma



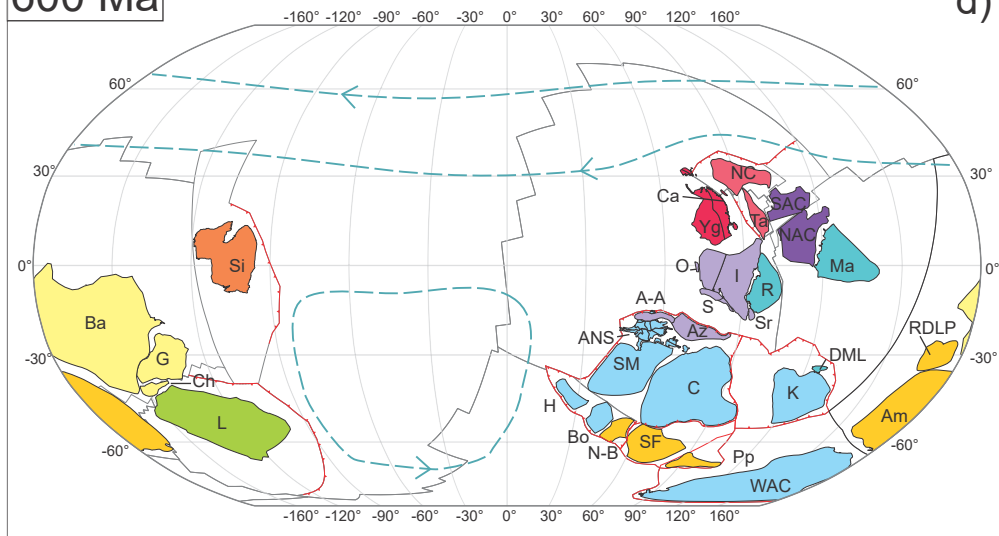
c)

750 Ma



b)

600 Ma



d)

